ADVANCING EARTH AND SPACE SCIENCES

JGR Atmospheres

RESEARCH ARTICLE
10.1029/2025JD044798

Key Points:

- Wildfire smoke from fires in Canada moved over NYC. The plume remained in the lower troposphere as it was advected over the city
- The daily cycle of fire intensity in Quebec likely contributed to the daily cycle of $PM_{2.5}$ concentrations in New York City
- An extremely slow-moving extra-tropical cyclone advected the smoke from Quebec to New York City for three straight days

Supporting Information:

Supporting Information may be found in the online version of this article.

Correspondence to:

G. S. Randazzo,
grandazzo@ccny.cuny.edu

Citation:

Randazzo, G. S., Hill, S. A., Booth, J. F., & Field, R. D. (2026). A wall of smoke: Understanding the drivers of the June 2023 Canadian wildfire smoke event for New York City. *Journal of Geophysical Research: Atmospheres*, *131*, e2025JD044798. https://doi.org/10.1029/2025JD044798

Received 8 JUL 2025
Accepted 3 APR 2026

Author Contributions:

Conceptualization: Gregory S. Randazzo, Spencer A. Hill, James F. Booth
Formal analysis: Gregory S. Randazzo
Methodology: Gregory S. Randazzo, Spencer A. Hill, James F. Booth
Project administration: Spencer A. Hill, James F. Booth
Supervision: Spencer A. Hill, James F. Booth
Visualization: Gregory S. Randazzo
Writing – original draft: Gregory S. Randazzo
Writing – review & editing: Gregory S. Randazzo, Spencer A. Hill, James F. Booth

A Wall of Smoke: Understanding the Drivers of the June 2023 Canadian Wildfire Smoke Event for New York City

Gregory S. Randazzo[1], Spencer A. Hill[1], James F. Booth[1], and Robert D. Field[2,3]

[1]Department of Earth and Atmospheric Sciences, City College of the City University of New York, New York, NY, USA, [2]Department of Applied Physics and Applied Mathematics, Columbia University, New York, NY, USA, [3]NASA Goddard Institute for Space Studies, New York, NY, USA

Abstract The 2023 Canadian wildfire season was notable for its extent and the dense smoke it produced. Motivated by the resulting record-breaking air quality hazard in the New York City region, we use in situ observations, satellite retrievals, reanalysis data, and trajectory analysis to explore how the smoke aerosol emitted from the Quebec fires came to influence $PM_{2.5}$ concentrations ~1,000 km downstream in New York City. Using emissions estimates from the Regional Advanced Baseline Imager + VIIRS Emissions data set and injection height estimates from the Integrated Monitoring and Modeling System, we relate the emissions timing of the fires with the broader synoptic context and surface $PM_{2.5}$ concentrations. The smoke aerosols were predominantly confined to the boundary layer and lower troposphere throughout the event. The daily cycle of fire emission intensity contributed to sub-daily variations in $PM_{2.5}$ concentrations in New York City downstream. Using data from the NYS Mesonet Profiler Network, radiosondes, and ERA5 reanalysis, we clarify the critical role played by a strong, quasi-stationary extratropical cyclone east of the fires: this cyclone's unusually slow, westward propagation helped organize the plume and advect its smoke from Quebec to New York City for three consecutive days.

Plain Language Summary Canada's 2023 wildfire season broke many records, and over June 6–8 the smoke produced by fires in Quebec came to New York City nearly 1,000 km downwind. Motivated by the resulting record-breaking $PM_{2.5}$ concentrations values in this city, this study uses satellite observations, ground-based measurements, reanalysis data, and trajectory analysis to better understand this historic wildfire smoke transport event. We demonstrate that a strong, very slow-moving extratropical cyclone east of the fires played a key role in transporting and confining the smoke over the region. We also find evidence that the peak in fire intensity occurring each afternoon within Quebec contributed to sub-daily $PM_{2.5}$ peaks downstream in the city. These results underscore the importance of synoptic-scale circulation in facilitating long-range smoke transport and highlight the potential for distant wildfire activity to drive severe air quality events in urban areas.

1. Introduction

In the summer of 2023, there were record-breaking burned area (Jain et al., 2024) and smoke emissions (Byrne et al., 2024) from Canadian wildfires. Among other impacts, the resulting smoke degraded air quality in parts of Canada and the northeastern US. For New York City (NYC), smoke originating from fires in Quebec in early June fueled record-poor air quality that was more hazardous than anywhere else in the world (Favetta, 2023). Within the event, which transpired over June 6–8, 2023, hourly concentrations of sub-2.5-micron particulate matter ($PM_{2.5}$) in Queens peaked above 400 μg/m^3 on the afternoon of June 7th and more generally comprise the six highest hourly values of the hourly $PM_{2.5}$ in the observational record, which starts in 2014 (Figure 1). Daily average $PM_{2.5}$ values in Queens on June 6th, 7th, and 8th respectively were 97.6, 200.4, and 115.1 μg/m^3, far exceeding the National Ambient Air Quality 24-hr standard of 35 μg/m^3. Nevertheless, within this event hourly $PM_{2.5}$ values varied by roughly an order of magnitude (Figure 1a).

Several studies of this event have investigated the smoke transport and impacts. Wang, Huang, et al. (2024) found using 3D aerosol modeling that the radiative forcing from "smoke shading" was negative at the surface, which led to an enhancement of the wind circulation. Kelesidis et al. (2025) estimated a daily mean surface temperature reduction of 3°C in Central Park. In terms of smoke origin, Magaritz-Ronen et al. (2025) noted in their trajectory-based analysis that fires in Western Canada contributed to enhanced carbon monoxide (CO) aloft over New York, but smoke at the surface mainly came from fires in Quebec. The large-scale circulation during the wildfire indicates that advection of the smoke involved an extratropical cyclone (ETC) that was centered over Nova Scotia

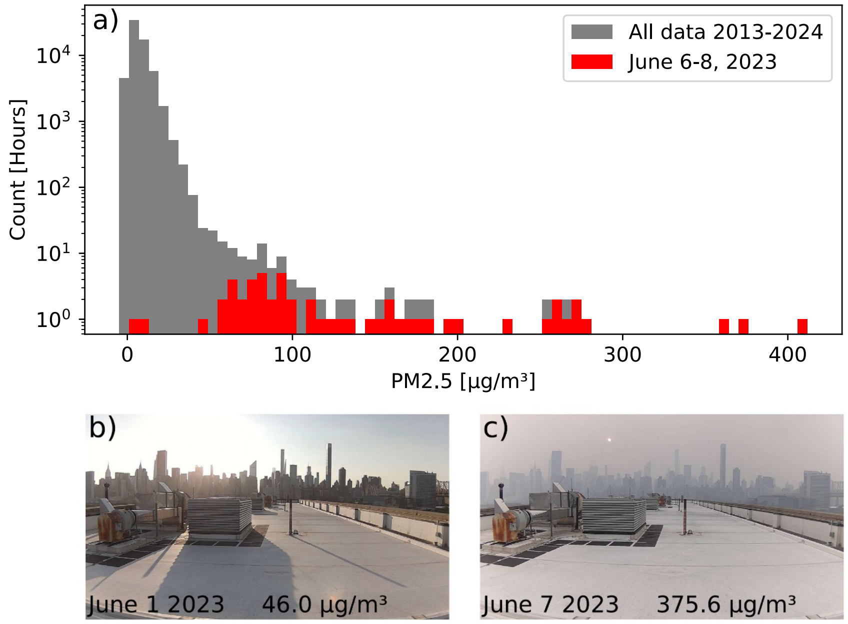

Figure 1. (a) Histogram of hourly concentrations of $PM_{2.5}$ from the Queens AirNow site from 1 January 2014 to 1 January 2025. Red values highlight June 6–8, 2023. (b, c) are images from Long Island City, Queens, New York, looking toward Midtown Manhattan on 1 June 2023 and 7 June 2023 at 7p.m. EDT (eastern daylight time). Particulate matter smaller than 2.5 microns concentrations ($PM_{2.5}$) in the images are from the Queens-Near Road measurement site at 7p.m. EDT from AirNow.

(Wang, Huang, et al., 2024; Zhu et al., 2024). Indeed, a true color composite from MODIS on June 6 shown in Figure 2 shows the wildfire smoke spanning New York state and a patch of bright clouds in the northeast portion associated with the ETC.

Our focus is on the extratropical weather patterns linking smoke emissions at the source in Quebec to hour-to-hour air quality changes 1,300 km downwind in New York City. We combine satellite retrievals, reanalysis data, ground-based aerosol profiles, in situ surface measurements, and trajectory analyses—a well-established methodology for understanding smoke transport over short (Su et al., 2025), medium (Colarco et al., 2004; Sapkota et al., 2005) and long ranges (Cottle et al., 2014; Shrestha et al., 2022; Sitnov et al., 2017). We specifically tried to answer:

1. How did the timing and injection height of smoke emissions in Quebec influence hourly order-of-magnitude changes in surface-level $PM_{2.5}$ concentrations in NYC?
2. What characteristics of the synoptic dynamics led to the extreme air quality conditions in NYC relative to typical patterns?

2. Data and Methods

2.1. Observations

Table 1 summarizes all in situ and remote sensing data sets used.

To track smoke emissions, we use total particulate matter (TPM) data from the Regional Advanced Baseline Imager (ABI) and Visible Infrared Imaging Radiometer Suite (VIIRS) fire Emissions (RAVE) database (Li et al., 2022) from 1 to 20 June 2023. RAVE calculates fire radiative power (FRP) over North America by combining two FRP measurements, one from active fire detections from the ABI on the Geostationary Operational Environmental Satellites R Series (GOES-R), and another with higher resolution (375 m) from VIIRS. It then uses land-cover specific emissions parameters to estimate total particulate matter emissions. RAVE has been shown to compare well with satellite observations (Li et al., 2022). To approximate plume injection heights from 4 to 6 June 2023, we use an estimate from the Integrated Monitoring and Modeling System for wildland fires (IS4FIRES). IS4FIRES calculates plume height with satellite-derived FRP assimilated by the Copernicus

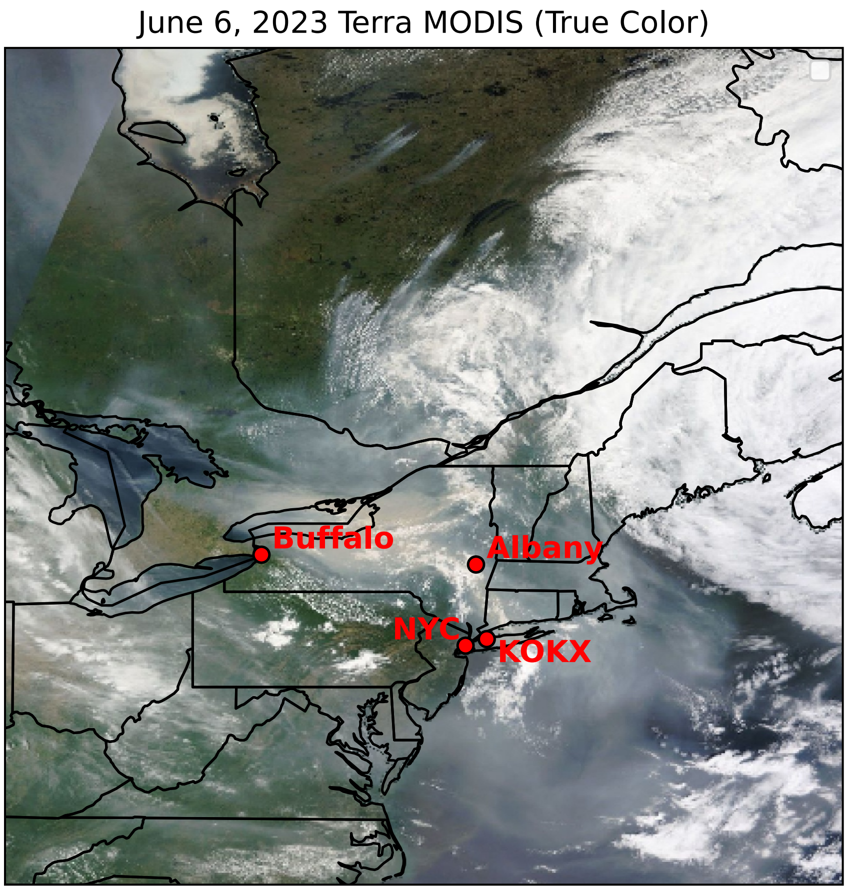

Figure 2. MODIS True Color Image from 15:35Z 6 June 2023. The plume is darkest between Albany and Buffalo. It stretches from the region of the fires in Quebec, across the eastern U.S. and over the Atlantic. The eastern side of the plume is embedded within a large cloud mass.

Atmosphere Monitoring Service (Rémy et al., 2017; Sofiev et al., 2012) at 0.1° × 0.1° horizontal resolution. IS4FIRES uses 1-km FRP from the MODIS Terra and Aqua active fire products, meteorological fields from ECMWF forecasts, and a semi-empirical parameterization to estimate plume injection heights. To compensate for the MODIS overpass being in late morning, versus the fire intensity peak typically being in late afternoon, IS4FIRES uses the maximum 1-km FRP value within each 0.1° × 0.1° grid cell rather than the grid-cell mean

Table 1
Data sets Used, With Variables, Resolution, Domain, and Study Period

Data set	Variable(s)	Spatial res.	Temporal res.	Domain and period
AirNow	$PM_{2.5}$ [μg/m^3]	N/A	Hourly	Queens, Albany, Buffalo NY May 29–June 20)
RAVE Emissions	TPM emissions [kg]	3 km	Daily	N.E. US, E. Canada (1–20 June)
IS4FIRES	Plume injection height [m]	0.1° × 0.1°	Daily	N.E. US, E. Canada (4–6 June)
ERA5 Reanalysis	MSLP, u, v, ω, Z500	0.25° × 0.25°	3-hourly	Global, N.E. US focus (1–20 June)
ERA5 Climatology	Daily SLP, MSLP, Z500	0.25° × 0.25°	Daily	Global (1950–2010)
MERRA-2	BC, aerosols	0.5° × 0.625°, 72 levels	Hourly	Global (1–20 June)
LAGRANTO	Parcel trajectories	ERA5 native	Hourly	E. North America (5 June +96hr)
MODIS Imagery	Smoke structure	1 km	Daily comp.	E. North America (1–20 June)
NYS Mesonet LiDAR	CNR (100 m–7 km)	Point profiles	5 min	Buffalo, Queens (1–20 June)
U. Wyoming Radiosonde archive	T, RH, inversions	Soundings	12-hourly	Buffalo, Long Island (4–9 June)

value. Both the RAVE emissions data and IS4FIRES injection heights carry uncertainties associated with satellite FRP retrievals and vegetation-specific emission data sets. The IS4FIRES plume injection heights further depend on a plume rise parametrization of plume buoyancy and entrainment. These parameterizations carry uncertainties in the satellite based radiance data and land parameters used to initialize them. We use NASA Moderate Resolution Imaging Spectroradiometer (MODIS) True Color imagery to document the structure of the smoke plume and track its position in relation to surrounding weather systems.

To analyze surface $PM_{2.5}$, we use data from the AirNow New York State Department of Environmental Conservation (NYSDEC) Air Quality Monitoring Network (https://dec.ny.gov/environmental-protection/air-quality/monitoring). Hourly NYSDEC surface $PM_{2.5}$ concentrations from 1 to 20 June 2023 in New York City, Albany, and Buffalo were obtained via the EPA's Air Quality System (AQS) application programming interface (http://airnowapi.org/).

To examine the vertical position and motion of the plume, we use data from WindCube 100S Doppler LiDARs from Buffalo, New York and the Queens borough of New York City via the New York State Mesonet (NYSM) profiler network. These instruments detect backscattering from aerosols to generate vertical profiles of the carrier-to-noise ratio (CNR), which is proportional to backscattering (Shrestha et al., 2021). Shrestha et al. (2021) found a strong linear relationship between CNR values at 100 m above ground level and surface $PM_{2.5}$ concentrations. We use radiosonde data from Buffalo and Long Island for 4–9 June 2023 to identify atmospheric inversions (https://weather.uwyo.edu/upperair/sounding.shtml).

2.2. Reanalysis

For the synoptic analysis, we use 3-hourly meteorological values from the ECMWF Atmospheric Reanalysis version 5 (ERA5; Hersbach et al., 2020) of mean sea level pressure, zonal wind (u), meridional wind (v), vertical velocity on pressure levels (ω), planetary boundary layer height, and geopotential heights at 500 hPa (Z_{500}). The native horizontal resolution of ERA5's numerical model is approximately 31 km, and we use data output from ECMWF interpolated to a $0.25° \times 0.25°$ grid. Climatological anomaly fields for mean sea level pressure (SLP) and Z_{500} were calculated using daily mean ERA5 fields from 1981 to 2010 with a centered 5-day running mean.

We also examine a four-dimensional rendering of the plume using the Modern-Era Retrospective Analysis for Research and Applications version 2 (MERRA-2) reanalysis (Gelaro et al., 2017). MERRA-2 provides vertically resolved mixing ratios of aerosol species from both natural and anthropogenic sources, with black carbon species divided into hydrophilic and hydrophobic components. For this study period, it directly assimilates biomass emissions from the Quick Fire Emission Data set, version 2.4r6 (Darmenov & da Silva, 2015) as well as aerosol optical depth to generate estimates of vertical aerosol distributions (Randles et al., 2017).

2.3. LAGRANTO Trajectory Model

To study air mass transport, we use the LAGRANTO trajectory model (Sprenger & Wernli, 2015). LAGRANTO is a Lagrangian analysis tool which solves for air parcel trajectories by interpolating gridded wind fields from ERA5 in space and time and applying a time-stepping scheme to advance parcel positions. We initialized the LAGRANTO trajectory model using the set of pixels with positive TPM values within a box covering southern Quebec on 12Z 5 June 2023 at the altitudes of injection heights from IS4FIRES. We convert injection heights to pressure values using daily mean surface pressure from ERA5, and run the model for 96 hr, using the ERA5 meteorological fields p, u, v, and ω at $0.25° \times 0.25°$grid resolution. LAGRANTO calculates the vertical motion of air parcels on pressure levels at the native vertical resolution of ERA5. LAGRANTO operates similarly to HYSPLIT's trajectory model, but offers additional features and straightforward usage of ERA5 data.

2.4. ETC Tracking

An extratropical cyclone (ETC) impacted the wildfire smoke transport on June 6–8, 2023, and we will examine this in detail in the results section. As part of the examination, we analyze the track of the ETC as compared to other ETC tracks. We generate the ETC tracks by applying the MAP Climatology of Midlatitude Storminess (MCMS) algorithm (Bauer & Del Genio, 2006) to SLP fields from ERA5 reanalysis. MCMS is a tracking algorithm designed for ETCs (Bauer et al., 2016). The SLP data we use is 6-hourly and spans 1950–2023.

The tracker has two main steps: (a) finding low-pressure centers globally, and, (b) connecting centers together in time to make tracks. The connection algorithm utilizes synoptic meteorology insights to determine which low-pressure centers to connect in time. MCMS has been utilized for multiple analyses of ETCs (e.g., Booth et al., 2017).

The ETC track statistics we focus on are track-averaged forward speed and track trajectory. We calculate forward speed as the distance traveled, using great circles, by the low-pressure center of the cyclone per 6-hourly timestep. For each cyclone, we average the 6-hourly forward speeds for all points along the track that fall within our 1,000-km circle. We calculate track trajectory as vector that the track path creates then the ETC passes through a specific study region. The vector angle is defined by the starting point and ending point for the track path through a specified region. The vector magnitude is defined as the mean track forward speed for all points within the specified region. Our specific regions are circles of radius 1,000 km spaced across the study domain.

3. Results

3.1. Surface Observations and Trajectory Analysis

In this subsection we will show that the total particulate matter emissions from wildfires in Quebec exhibit a strong daily cycle from 4 to 6 June and that this smoke remained in the lower troposphere as it was advected over the Northeast U.S. including New York City.

Figure 3a shows the smoke production in southern Quebec, as indicated by the hourly time series of area-averaged TPM from RAVE over the box shown in Figure 4. From June 4th–6th, increasing daily peak TPM values, along with the increasing area of pixels with positive TPM values (not shown), indicate that the fires proliferated and expanded rapidly. This smoke was then advected to New York State, first to locations upstream of NYC such as Buffalo (Figure 3b) and then to NYC (Figure 3c). This can be seen from the dotted curve in Figure 4, which is the mean forward trajectory of parcels starting at the locations of the fires from 12Z June 5 to 12Z June 9. These parcels traveled south south-west, then curved toward the east as they crossed into New York. The full set of trajectories, each initialized at the location and height of one of the identified plume sources, suggests that virtually all of the parcels from the fires followed a semi-elliptical trajectory over the 96-hr period that brought them over or near New York City (Figure S1 in Supporting Information S1).

Based on the AirNow surface $PM_{2.5}$ data, this advected wildfire smoke led to record high $PM_{2.5}$ values in New York City. On 7 June 2023, $PM_{2.5}$ concentrations in Queens exceeded 400 μg/m^3—the highest recorded since at least 2014 (Figure 1a). The daily $PM_{2.5}$ concentration for New York City, defined as the mean of hourly measurements across NYC sites, was above 100 μg/m^3. In upstate New York (Figure 3b), Albany and Buffalo also experienced hourly maximum $PM_{2.5}$ values above 100 μg/m^3.

Smoke concentrations in NYC exhibited strong sub-daily variability, with $PM_{2.5}$ peaks in the afternoon on June 6th, 7th, and 8th (Figure 3c). A possible contributing factor to these peaks were daily late afternoon peaks in the fire emissions upstream (Figure 3a): all else equal, including the advection timescale, this would lead to roughly equally spaced peaks downstream. The three arrows in Figure 4c represent the times it took for trajectories initialized from the daily mean fire locations on June 4th, 5th, and 6th to cross the approximate longitude of NYC (73.97 W). The parcel initialized on June 4th does arrive at NYC approximately one day later, near the time of the 5 June $PM_{2.5}$ peak. However, the June 5th parcel takes roughly twice as long as either those on the 4th or 6th, such that the mean June 6th parcel arrives at NYC just a few hours after the mean June 5th parcel. This would help explain the severity of the June 7th NYC $PM_{2.5}$ peak, but not the June 6th peak. Many other mechanisms, including the diurnal cycles of boundary layer processes and secondary aerosol evolution could meaningfully influence the sub-daily $PM_{2.5}$ timing. Still, we infer from these time series that the daily late-afternoon fire intensity peaks did play some role in the hourly surface $PM_{2.5}$ variability downstream in NYC.

The distribution of estimated plume injection heights for 5th–7th June from IS4FIRES (Figure 5) suggest that the smoke plume at the source of the fires was mostly contained in the lower troposphere. The maximum plume injection heights in the area (box in Figure 4) from 5th to 7th June reached slightly over 3 km, and the mean injection heights were below 2 km. These are considerably lower than those of a July 2002 event of wildfire smoke advection from Quebec to the Northeastern U.S., in which injection heights were estimated to be ∼2–6 km (Colarco et al., 2004). The histogram of injection heights in Figure 5 also reveals a somewhat bimodal structure,

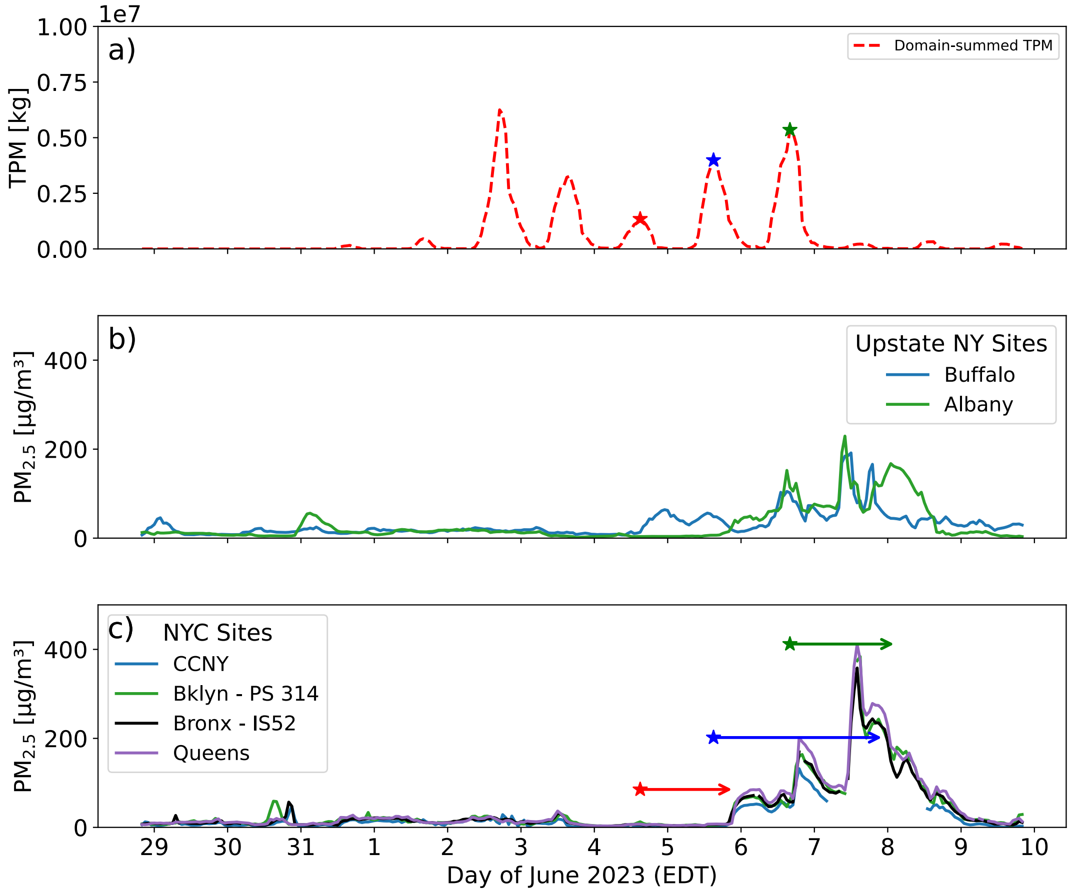

Figure 3. Total Particulate Matter (TPM) estimate, and surface particulate matter smaller than 2.5 microns ($PM_{2.5}$) at six locations in New York State from June 1–12, 2023. (a) The area sum of total daily particulate matter emissions from the hourly Regional ABI VIIRS Emissions (RAVE) Total Particulate Matter (TPM) estimate (RAVE TPM). The area over which the sum is taken is represented by the dashed box in Figure 4 (b) $PM_{2.5}$ from Buffalo and Albany, NY. (c) Solid lines show observations of $PM_{2.5}$ concentrations at four sites in New York City. Geographic locations of the $PM_{2.5}$ data sites are shown in Figure 2. All data are hourly and local time (EDT). Red, blue, and green stars are located at times of peak particulate matter emissions (from Figure 3a). Height of stars reflects heights of maxima in the Queens ($PM_{2.5}$) time series. Length of the arrows reflects the time it took for the mean parcel trajectory from June 4th, 5th, and 6th to cross the approximate longitude of NYC (73.97 W). Tick marks correspond to 12a.m.

with a minimum frequency of height per pixel occurring above the mean of the injection height distributions, and with moderate day-to-day variability over June 5th–7th.

On June 6th, a large gray-brown patch of wildfire smoke is located between Buffalo and Albany (Figure 2). The mean trajectory line calculated from June 5th (Figure S2 in Supporting Information S1) overlaps with the right edge of this area of concentrated smoke. Trajectories for the same set of points initialized on June 4th and 6th (Figure S2 in Supporting Information S1) show a mean trajectory further to the west, overlapping regions of northeast Pennsylvania and central New Jersey. This indicates that the trajectory of smoke parcels which were emitted around June 5th 12Z were "aimed" toward New York City as the flow pattern shifted.

NYSM Profiler network Doppler LiDAR CNR profiles in Figure 6 show the time-evolving vertical structure of the smoke plume as it passed over Buffalo and Queens. The highest CNR values in Buffalo began midday on June 7th in a band at an altitude of approximately 1 km, with an increase in CNR at higher altitudes around midnight on the 7th and 8th. In contrast, the highest CNR values in Queens were closer to the surface (~100 m). The Queens CNR peaks occur at approximately the same time as the peak in surface $PM_{2.5}$ concentration, in the afternoon of June 7th.

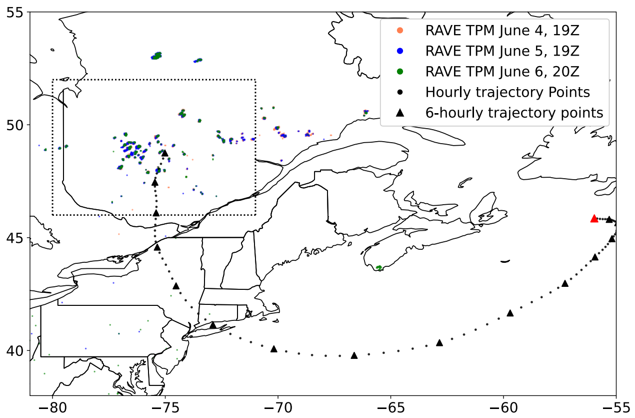

Figure 4. Regional ABI VIIRS Emissions (RAVE) Total Particulate Matter (TPM) estimate, and mean Lagranto trajectory. Colored markers indicate locations of particulate matter emissions from the Quebec wildfires for the period June 4–6 at their hour of maximum intensity. The dotted line indicates the mean trajectory of parcels from the emissions sources from 5 June 2023 12Z to 9 June 2023 12Z. The parcels were initialized at the locations of the emissions at an altitude of their respective plume injection height. The LAGRANTO trajectory model traced the path of air parcels within the smoke plume using the ERA5 reanalysis.

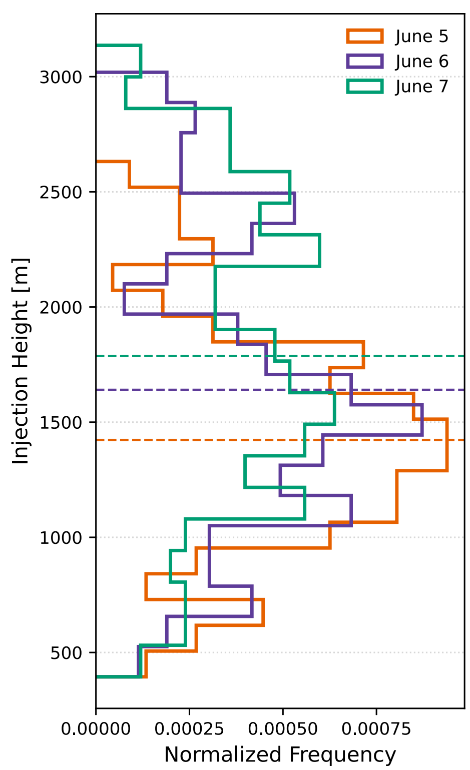

Figure 5. Normalized daily area-averaged injection height frequency estimate from IS4FIRES from June 5–7, 2023. The distribution was calculated over the box in Figure 4. The dashed lines represent the means for each distribution.

Throughout the episode, the CNR profiles indicate that smoke in both Buffalo and Queens was confined to the lower troposphere. Combined with the $\lesssim$3 km injection heights of the smoke plumes described above, this suggests that the smoke aerosol came to NYC predominantly via horizontal advection—a "wall of smoke." This contrasts with the 2002 event, in which downward transport of initially lofted smoke particles was central (Colarco et al., 2004).

Atmospheric sounding data from KBUF (Buffalo) and KOKX (Long Island) shown in Figure 7 suggests that temperature inversions contributed to preventing the smoke from dispersing via mixing aloft. At both stations, a set of weak lower tropospheric inversions between 850 hPa and the surface exists on June 4–6, along with a more pronounced surface inversion on June 7–9. Though turbulent flow below the inversion may have contributed to localized downdrafts (Figure S3 in Supporting Information S1), downdrafts within the boundary layer in Queens do not in general correspond in time to $PM_{2.5}$ peaks and do not seem to diminish CNR values aloft. In particular, the spike in $PM_{2.5}$ exceeding 300 μg/m^3 in Queens on June 7 (Figure 3c) is simultaneous with the sudden appearance of a fairly homogenous aerosol layer in the CNR data extending from the surface to nearly 4 km (Figure 6b). This again seems more readily explained by horizontal advection of the plume throughout the lower troposphere rather than vertical advection or mixing.

3.2. Synoptic View

The MODIS imagery for June 5–7 in Figures 8a–8c shows a comma-shaped cloud system typical of an extratropical cyclone, centered off Nova Scotia. The smoke plume moved within the cyclone's drier, cold sector—the band of clouds associated with the cold front's edge can be seen downstream of the plume on the 7th. This position within the dry, cold sector contributed to a lack of appreciable precipitation along the track (Figure S4 in Supporting Information S1), resulting in little wet deposition of the smoke aerosol between Quebec and NYC.

Based on ERA5 mean sea level pressure (SLP) in Figures 8e and 8f, from June 5 to June 7 the cyclone's SLP minimum deepened by ∼2 hPa while shifting only a few degrees longitude; as detailed below this is atypical for ETCs in this region (Booth et al., 2017). The cyclone's northerly flow to the west of the SLP minimum strongly determined the overall southward trajectory of the smoke plume from Quebec, funneling it toward the northeast US. The low had previously pinched off from the surface pressure field and deepened through this period, which explains the acceleration in the flow seen in the trajectory analysis (see hourly positions of mean trajectory in Figure 4).

Figure 9 shows the evolution of the 500-hPa geopotential height field from the 4th to the 9th over the whole North American domain. The low-pressure center remains quasi-stationary throughout the study period, as upstream flow is limited by the presence of an omega block over central North America (Figure 9a). This persistent period of northerly flow allowed the smoke plume to remain organized by the time it had reached New York City on the 7th. Both the ETC associated with smoke transport and the upstream omega block extended vertically throughout the troposphere. From the perspective of the 500-hPa field (Figure 9), the low had already been well formed by the 4th, situated on the right side of the omega block. The block deepened to its maximum intensity on the 5th. Subsequently, the upper-level low deepened, reaching its maximum extent on the 7th. However, the surface low reached its maximum intensity on the 6th. The temporal persistence of the upper level

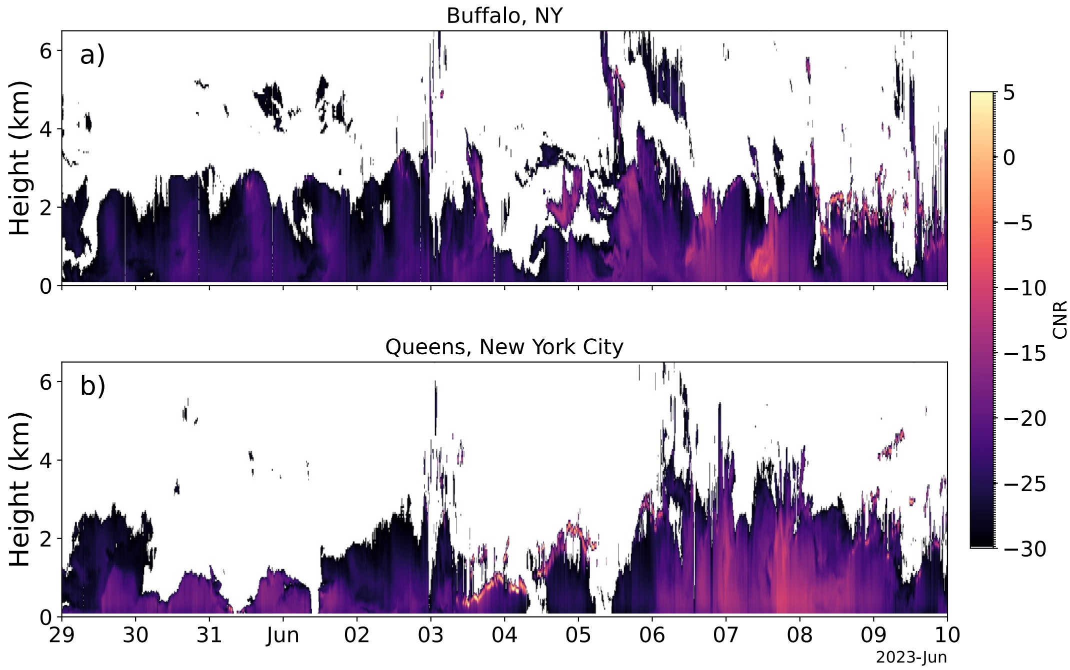

Figure 6. Carrier-to-noise ratio (CNR) from the New York State MESONET LiDAR Profiler network in panel (a) Buffalo and (b) Queens, New York City. Higher values of CNR indicate higher aerosol backscattering. May 29 to 10 June 2023. The time is UTC.

and surface low, and its position near New Brunswick, Canada were critical in enabling the wildfire smoke to be advected south. Additionally, the persistence of the high over the center of North America likely blocked the zonal flow which would have otherwise moved the Northeastern low out of the domain much sooner.

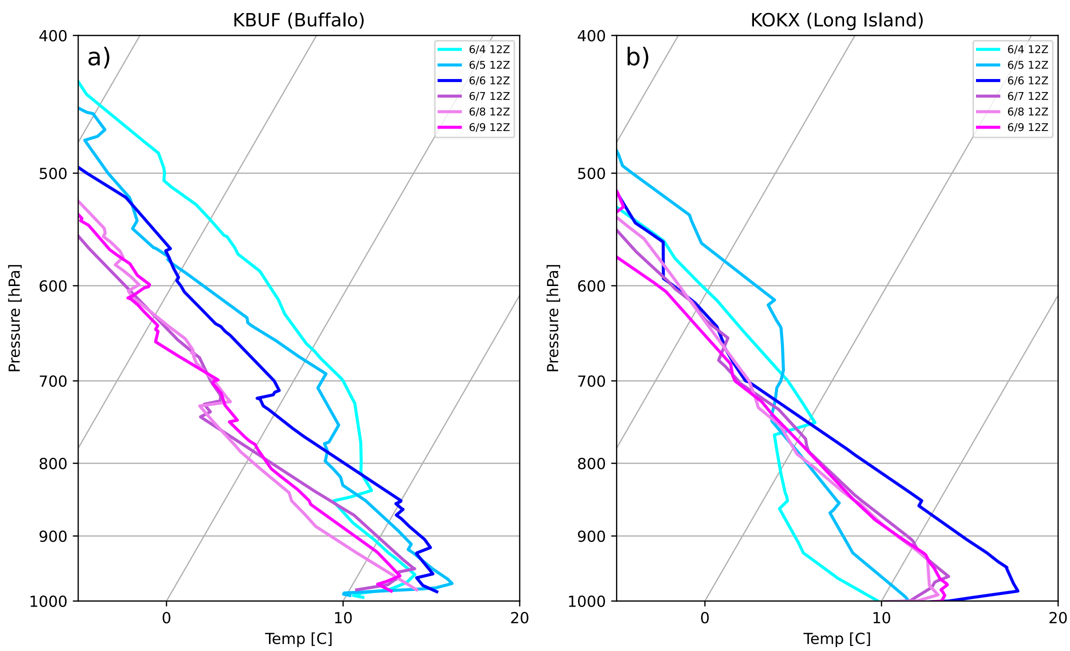

Figure 7. Atmospheric sounding data from (a) KBUF (Buffalo) and (b) KOKX (Long Island) from the NOAA National Centers for Environmental Information via the University of Wyoming Atmospheric Science Radiosonde Archive https://weather.uwyo.edu/upperair/sounding.shtml.

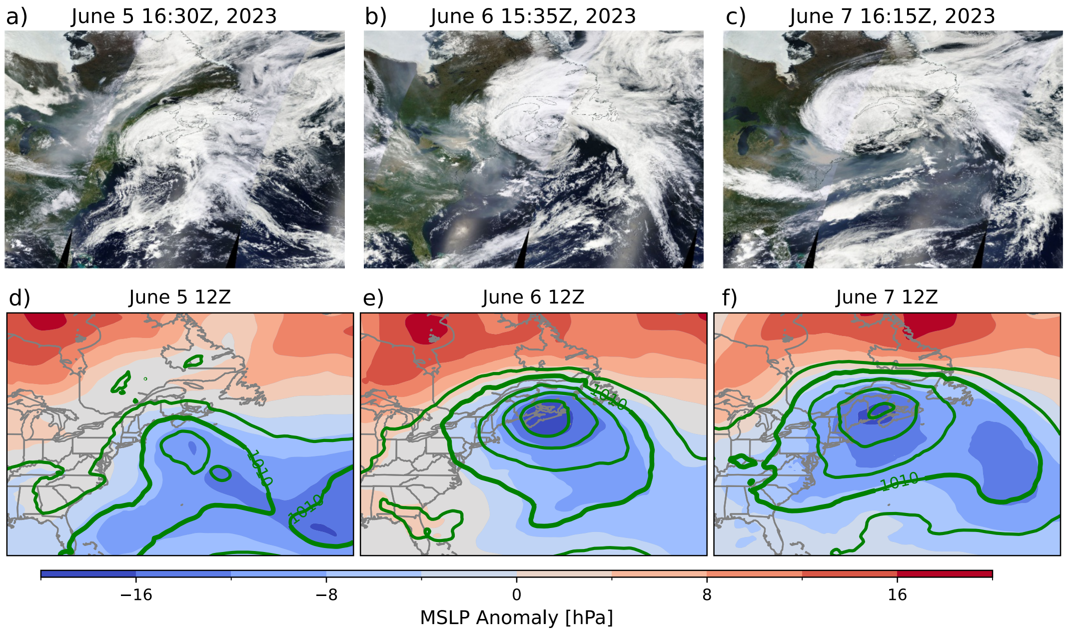

Figure 8. (a–c): MODIS True Color image imagery June 5–7. (d–f): mean sea level pressure (MSLP) (contoured) and MSLP anomaly (shaded) with respect to 1981–2010. Times in the title represent the leftmost swath for the 5th and 7th, and the center swath for the 6th. Times for the right swath on the 5th and 7th are 14:54Z and 14:37Z respectively. The contour interval for MSLP is 5 hPa.

Figure S5 in Supporting Information S1 shows a time series of area-mean meridional flow in the lower troposphere (box in Figure 11c). From June 1st to 11th, there was northerly flow aloft. A weakening of the northerly flow associated with the eastward movement of the low is clear from the 7th–9th. From the 12th to the 15th, there was southerly flow. This southerly flow explains why TPM emissions in Figure 3a do not translate into surface $PM_{2.5}$ peaks in New York City during this time period. Northerly flow associated with the low that carried the smoke toward New York City on June 7th is present from June 4th–June 9th. TPM peaks in Figure 3a in early June

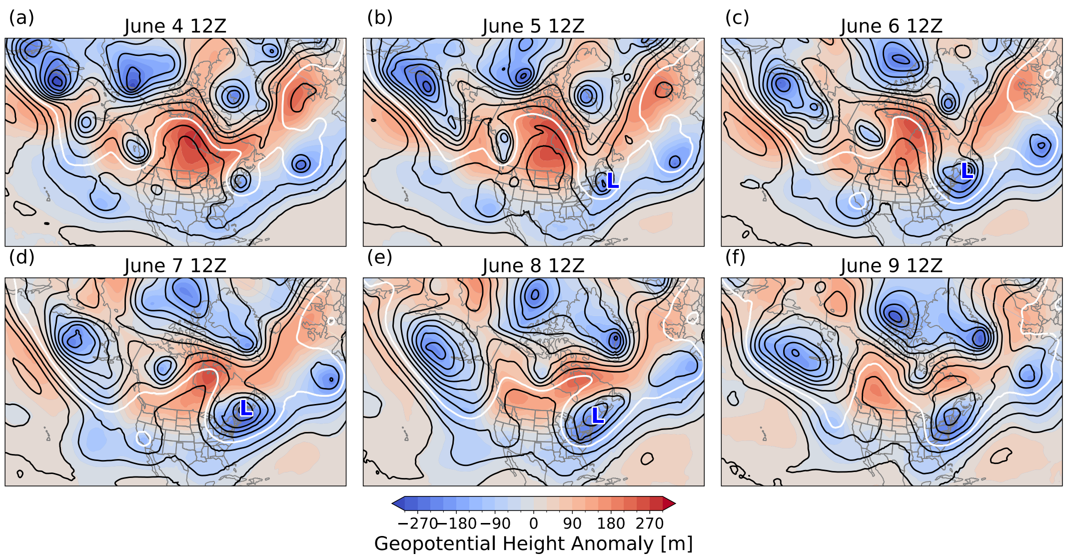

Figure 9. Z500 (shaded) and Z500 anomaly (contoured) The contour interval is 60 m, and the white index contour is at 5,400 m. The Ls in panels (b–e) indicate the locations of a surface low pressure system detected by the MCMS extra-tropical cyclone (ETC) tracking algorithm. This low is associated with the smoke transport toward the Northeast U.S. An omega block in the center of North America is present through this period.

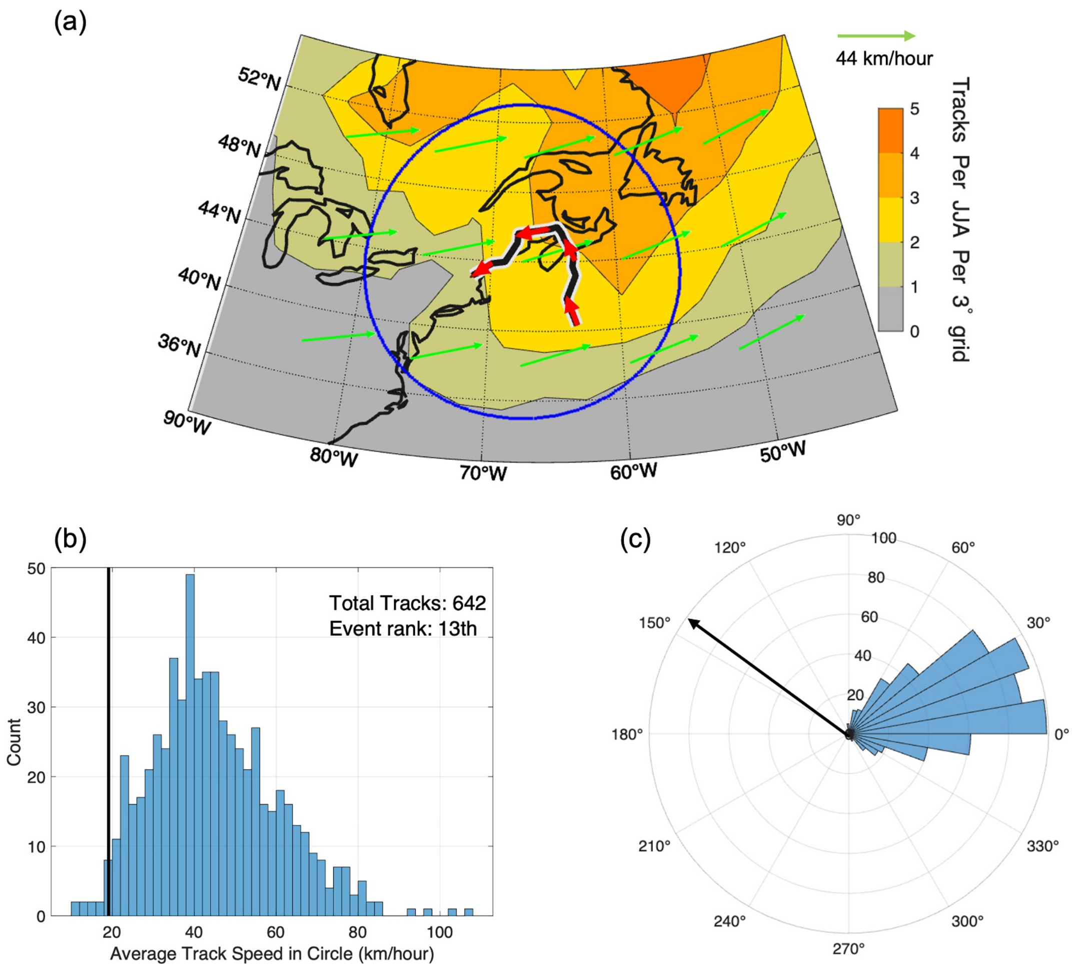

Figure 10. Extratropical cyclone (ETC) statistics. (a) Shaded: mean June-August ETC track density from 1950 to 2023 for all tracks passing through the region (total ETC tracks: 1712). Black line the track path of the cyclone for the 2023 smoke event from 12Z June 4th to 18Z June 8th. Red arrows indicate direction of the ETC. Green vectors show the average track trajectory for all ETCs within 1,000 km radius of the base of each vector. The blue circle radius is 1,000 km, centered on 44°N, 67.5°W. (b) Mean forward speed for each ETC that spent at least 18 hr within the blue circle. The speed for the ETC that impacted the wildfire smoke event is indicated by the black vertical line. (c) Histogram of track trajectories of the ETC that passed through the circled region. The track trajectory for the wildfire smoke ETC is 145°, and the length of the arrow is arbitrary. The convention used for the angle directions in the stereographic plot are those used most commonly in mathematics.

are not associated with any features in the New York City time series, because at that time, the storm which carried the smoke had not yet formed (Figure S6 in Supporting Information S1); instead, the surface high to the north of the event was generating strong westward advection over the fire region.

Figure 10 demonstrates the uniqueness, in terms of storm speed and storm path, for the extratropical cyclone (ETC) that was the critical to the southeastward advection of wildfire smoke from June 6–8. The ETC formed over the Atlantic at 12Z on June 4 and moved northwest and over Nova Scotia. Then the storm traveled southwest along the coast (black line with red arrows showing track direction, Figure 10a). This travel path is not expected for the region. The mean track trajectories per 1,000 km region (green vectors Figure 10a) demonstrate that most ETCs travel east by northeast as they move through the region.

This ETC was also moving extremely slowly in terms of the forward speed of the low-pressure center (Figure 10b). For the 72 years of ETC tracks analyzed, we found that 642 storms passed within 1,000 km of the centroid region of the June 2023 ETC (i.e., 44°N by 67.5°W). The storm that impacted the wildfire was in the bottom 2% in terms of track speed for ETCs that pass through this region in the summer.

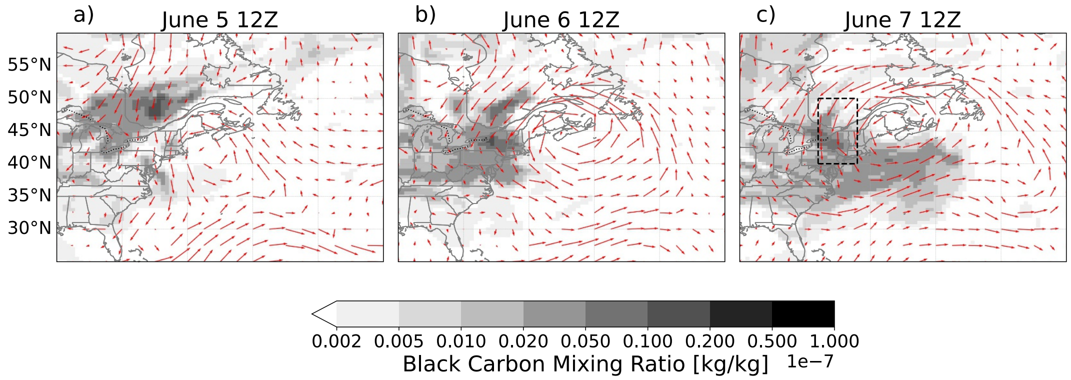

Figure 11. (a–c): Grayscale indicates the column integrated black carbon mixing ratio (hydrophilic + hydrophobic) from MERRA-2, along with winds at 900 hPa from ERA5.

Given that the track paths of ETCs can vary significantly, Figure 10c is included to show that the mean track trajectories shown in Figure 10a represent the majority of ETCs. In this case, we plot the angle component of our track trajectory metric in a stereographic histogram for the same subset of ETCs analyzed in Figure 10b. This histogram demonstrates that the path track angle taken by the June 2023 event was also extremely rare.

3.3. MERRA-2 Analysis

Figure 11 shows the black carbon mixing ratio at approximately 900 hPa from the MERRA-2 reanalysis with 900 hPa horizontal winds from ERA5 overlaid. On June 5th, the plume is stretched along a northeast-southwest axis by northeasterly flow, as it is situated between the surface low and a higher pressure system to the northwest. Embedded within the plume is an area above the surface fires with elevated black carbon levels compared to the rest of the plume, near the location of the fires. By the 6th and 7th, the majority of the plume is embedded within the northerly flow associated with the surface low (Figure 11a). These black carbon features qualitatively match the form of the plume from satellite imagery (Figures 8a–8c).

We do not attempt to validate the vertically resolved black carbon mixing ratios from MERRA-2 which are used to produce the column-integrated product. However, a comparison between an estimate of surface $PM_{2.5}$ based on column-integrated aerosols from MERRA-2 and surface observations in NYC (Figure S7 in Supporting Information S1) reveals that, while MERRA-2 shows elevated $PM_{2.5}$ values for three days, concurrent with the event, it does not capture the timing and underestimates the magnitudes of the daily peaks, particularly the 12 hr on June 7th when observed $PM_{2.5}$ exceeded 200 $\mu g/m^3$. Assuming that higher confidence can be associated with MERRA-2's meteorological assimilation, the discrepancy is possibly due to limitations of the biomass burning emissions data set which drives MERRA-2, primarily in its daily mean temporal resolution (Randles et al., 2017).

4. Discussion of Links to Prior Studies and Smoke Plume Events

The relationship between atmospheric blocking and downstream air quality impacts for the 2023 Canadian wildfire season was also investigated by Chen et al. (2025). For the western U.S., they identified a smoke transport pathway generated by northerly flow associated with the Alaskan Ridge and the Arctic High.

Magaritz-Ronen et al. (2025) use trajectory analysis with LAGRANTO and CO concentrations from the CAMS reanalysis, finding that CO from western Canada combined with CO from the Quebec fires before reaching New York City as a plume extending deep into the free troposphere. These findings regarding the longer-lived, gaseous CO are not inconsistent with our “wall of smoke” regarding smoke *aerosol*. In addition, though the smoke plumes may have started out well-mixed, it is likely that vertical density stratification within the plume concentrated particulate matter closer to the surface and lighter constituents such as CO toward the top.

Similar to the June 2023 plume, in July 2002 a large smoke plume was advected into the mid-Atlantic region from southern Quebec (Colarco et al., 2004), driven by a low over the Canadian maritime provinces and a high in the Great Lakes region, resulting in northerly flow that organized the plume and funneled the smoke south (Colarco et al., 2004). Synoptically, the 2002 event was similar to the 2023 event, in that the smoke was transported and concentrated between a high and a low, traveling within the cold sector of an extratropical cyclone. However, Colarco et al. (2004) contrast the 2002 case with those in which smoke from Canada reaches the Northeast U.S. at low altitudes through the cold front of a mid-latitude cyclone; they also show via numerical modeling that injection heights below 3 km were inadequate to explain observed surface mass for the 2002 event. Mixing from the free troposphere into the boundary layer was the primary explanatory mechanism for high surface $PM_{2.5}$ concentrations during this event.

Sapkota et al. (2005) use HYSPLIT and LiDAR measurements to study the July 2002 Quebec wildfires, and arrive at a similar conclusion to (Colarco et al., 2004). They demonstrate descent of a plume from a height of ∼1.5 km to the surface via a time series of range-corrected relative aerosol backscattering measurements. High $PM_{2.5}$ concentrations measured by the LiDAR are consistent with an increase from around 60 to 200 μg/m^3 in Baltimore.

Shrestha et al. (2022) documented a case in July 2021 where wildfire smoke from Western Canada was transported over New York State, resulting in poor air quality over the region. They utilized a combination of HYSPLIT trajectory analysis, and Doppler LiDAR carrier-to-noise ratio (CNR) to show that smoke mixing into the boundary layer via entrainment and subsidence from an initial height below ∼2.0 km caused $PM_{2.5}$ levels to spike across New York State.

Previous studies have utilized trajectory analysis and observations to document smoke transport events in other extratropical regions. Su et al. (2025) documented a case in 2019 of surface smoke advection across Virginia, and used a combination of HYSPLIT and LiDAR data to track the plume trajectory and vertical transport. Mixing into the boundary layer was identified by a downward sloping feature in the LiDAR backscattering. Sitnov et al. (2017) and Zheng et al. (2020) use trajectory analysis, along with satellite measurements of fire radiative power, to document a cases in 2016 and 2017 of long-range surface smoke advection in Siberia and over the Atlantic. Sitnov et al. (2017) used back trajectories from a location impacted by smoke to show that the plume remained in the lower 2 km of the atmosphere (Sitnov et al. (2017) Figure 5b) throughout its transport. Zheng et al. (2020) used LAGRANTO to document a case of wildfire smoke descending as a result of a dry-intrusion in the cold sector of an ETC. Cottle et al. (2014) documents a case in 2012 of long-range smoke transport from Siberia to British Columbia. Using back trajectories from model estimates of the fire sources, along with LiDAR observations, they show the subsidence of smoke from a height of 3 km in the free troposphere into the boundary layer, coincident with elevated $PM_{2.5}$ values at the surface.

Previous studies have also explored the relationship between fire locations, injection heights, emissions, boundary layer dynamics and synoptic flow, by primarily relying on either simulations (for e.g., Kochanski et al. (2019) or observational data. Modeling results from Kochanski et al. (2019) reveal that the smoke shading effect can enhance existing inversions and limit vertical mixing, while cooling the surface, limiting PBL growth. This can generate a positive feedback loop which results in enhanced smoke concentrations at the surface. They highlight that numerical weather prediction models often lack the ability to resolve this smoke-inversion feedback, leading to lower estimates of surface smoke concentrations. The strength of this feedback in the 2023 event for NYC is uncertain, however, the existence of a persistent inversion throughout the event warrants further investigation.

5. Conclusion

We have determined that for the Quebec wildfires in early June 2023, the smoke arrived in New York as a lower-tropospheric wall of smoke. This was different from other studies we are aware of, where smoke tended to be mixed from aloft down to the surface. A uniquely slow extratropical cyclone was instrumental in creating the meteorology that steered the wildfire smoke. The cyclone generated northerly flow which transported the smoke plume toward the Northeast US: whether initialized on the 4th, 5th, or 6th, forward trajectories initialized at the fire locations do not change substantially, reflecting the temporal persistence of the ETC. A large omega block over central North America likely contributed to this persistence of the ETC.

$PM_{2.5}$ measurements in New York City show a strong signal associated with the smoke from these fires, beginning on the 6th. Total particulate matter emissions from the fires exhibit a daily cycle, which is partially reflected in the variations in $PM_{2.5}$ observations in New York City downstream. The steadiness of the northerly flow allowed the hourly variations in fire activity in Quebec to imprint upon, though not completely dictate, hourly surface pollutant concentrations ∼1,000 km downstream in New York City. Injection heights from IS4FIRES indicate that most of the smoke was released in the lower troposphere, and observations from the

NYSM Doppler LiDAR network supports the presence of thick smoke aerosols below 2 km rather than descent of smoke from aloft.

Exposure to particulate matter from wildfire smoke is associated with respiratory morbidity, specifically for asthma and chronic obstructive pulmonary disease, and all-cause mortality (Keywood et al., 2015; Matz et al., 2020; Reid et al., 2016; Zu et al., 2016). In 2023 wildfire smoke emissions and transport (Jain et al., 2024; Wang, Wang, et al., 2024) caused significant health impacts across New York State, leading to an increase in asthma-related emergency department visits compared to the 2013–2022 baseline between June 1–14, 2023 (Meek et al., 2023). Our study has described the transport mechanism by which the smoke got from Quebec to New York, making use of hourly fire emissions estimates, trajectory analyses and synoptic weather analysis, but further analysis regarding the frequency of such events is required. While wildfire smoke concentrations are seasonally higher in western North America (Brey et al., 2018), the extremity of the 2023 Canadian wildfire season underscores the necessity of evaluating whether future changes to eastern wildfire activity could shift the eastern air quality regime toward one more typical of western North America. These changes will depend on shifts in transport patterns and upstream fire regimes, which through 2024 show moderate increases in burned area over eastern Canada (Hanes et al., 2025). There is significant uncertainty in projections of future burned area (Burton et al., 2024). For New York, we note that Curasi et al. (2024) project an increase centered over Ontario and Christian et al. (2023) suggest an increase in future flash drought frequency - and therefore fire potential - over the main region of 2023 burning in Quebec.

Conflict of Interest

The authors declare no conflicts of interest relevant to this study.

Availability Statement

AirNow $PM_{2.5}$ data can be obtained from http://airnowapi.org/. The NYSM Doppler LiDAR Profiler Network data is available via http://www.nysmesonet.org/ via request form (Brotzge et al., 2020; Shrestha et al., 2021). RAVE total particulate matter emissions can be obtained from https://sites.google.com/view/rave-emission/products?authuser=0. Plume injection height data (IS4FIRES) is available via https://doi.org/10.24381/a05253c7. MODIS True Color images can be downloaded from https://worldview.earthdata.nasa.gov/. Atmospheric sounding data can be obtained via the University of Wyoming Sounding Archive via https://weather.uwyo.edu/upperair/sounding.shtml. MERRA-2 reanalysis data can be obtained via https://doi.org/10.1175/JCLI-D-16-0758.1. ERA5 reanalysis data can be obtained from https://doi.org/10.1002/qj.3803. The LAGRANTO v2.0 trajectory analysis tool (Sprenger & Wernli, 2015) can be obtained via https://iacweb.ethz.ch/staff/sprenger/lagranto/index.html. GFAS data was obtained from the Copernicus Atmospheric Monitoring Service via https://ads.atmosphere.copernicus.eu/datasets/cams-global-fire-emissions-gfas?tab=overview (Copernicus Atmosphere Monitoring Service, 2022). Data and scripts for the figures can be accessed at: https://doi.org/10.5281/zenodo.15839152.

Acknowledgments

Thanks to Dr. Fred Moshary for providing crucial insights on interpreting LIDAR data.

References

Bauer, M., & Del Genio, A. D. (2006). Composite analysis of winter cyclones in a GCM: Influence on climatological humidity. *Journal of Climate*, *19*(9), 1652–1672. https://doi.org/10.1175/JCLI3690.1

Bauer, M., Tselioudis, G., & Rossow, W. B. (2016). A new climatology for investigating storm influences in and on the extratropics. *Journal of Applied Meteorology and Climatology*, *55*(5), 1287–1303. https://doi.org/10.1175/JAMC-D-15-0245.1

Booth, J. F., Dunn-Sigouin, E., & Pfahl, S. (2017). The relationship between extratropical cyclone steering and blocking along the north American East Coast. *Geophysical Research Letters*, *44*(23), 11976–11984. https://doi.org/10.1002/2017GL075941

Brey, S. J., Ruminski, M., Atwood, S. A., & Fischer, E. V. (2018). Connecting smoke plumes to sources using hazard mapping system (HMS) smoke and fire location data over North America. *Atmospheric Chemistry and Physics*, *18*(3), 1745–1761. https://doi.org/10.5194/acp-18-1745-2018

Brotzge, J. A., Wang, J., Thorncroft, C. D., Joseph, E., Bain, N., Bassill, N., et al. (2020). A technical overview of the New York state Mesonet standard network. *Journal of Atmospheric and Oceanic Technology*, *37*(10), 1827–1845. https://doi.org/10.1175/JTECH-D-19-0220.1

Burton, C. A., Kelley, D. I., Burke, E., Mathison, C., Jones, C. D., Betts, R. A., et al. (2024). Fire weakens land carbon sinks before 1.5°C. *Nature Geoscience*, *17*(11), 1108–1114. https://doi.org/10.1038/s41561-024-01554-7

Byrne, B., Liu, J., Bowman, K. W., Pascolini-Campbell, M., Chatterjee, A., Pandey, S., et al. (2024). Carbon emissions from the 2023 Canadian wildfires. *Nature*, *633*(8031), 835–839. https://doi.org/10.1038/s41586-024-07878-z

Chen, H., Zhang, W., & Sheng, L. (2025). Canadian record-breaking wildfires in 2023 and their impact on US air quality. *Atmospheric Environment*, *342*, 120941. https://doi.org/10.1016/j.atmosenv.2024.120941

Christian, J. I., Martin, E. R., Basara, J. B., Furtado, J. C., Otkin, J. A., Lowman, L. E. L., et al. (2023). Global projections of flash drought show increased risk in a warming climate. *Communications Earth and Environment*, *4*(1), 165. https://doi.org/10.1038/s43247-023-00826-1

Colarco, P. R., Schoeberl, M. R., Doddridge, B. G., Marufu, L. T., Torres, O., & Welton, E. J. (2004). Transport of smoke from Canadian forest fires to the surface near Washington, D.C.: Injection height, entrainment, and optical properties. *Journal of Geophysical Research*, *109*(D6), 2003JD004248. https://doi.org/10.1029/2003JD004248

Copernicus Atmosphere Monitoring Service. (2022). CAMS global biomass burning emissions based on fire radiative power (GFAS) [Dataset]. *ECMWF*. https://doi.org/10.24381/A05253C7

Cottle, P., Strawbridge, K., & McKendry, I. (2014). Long-range transport of Siberian wildfire smoke to British Columbia: LiDAR observations and air quality impacts. *Atmospheric Environment*, *90*, 71–77. https://doi.org/10.1016/j.atmosenv.2014.03.005

Curasi, S. R., Melton, J. R., Arora, V. K., Humphreys, E. R., & Whaley, C. H. (2024). Global climate change below 2°C avoids large end century increases in burned area in Canada. *npj Climate and Atmospheric Science*, *7*(1), 228. https://doi.org/10.1038/s41612-024-00781-4

Darmenov, A., & da Silva, A. (2015). The quick fire emissions dataset (QFED): Documentation of versions 2.1, 2.2 and 2.4 [Technical Report]., 32(NASA/TM–2015–104606).

Favetta, M. (2023). Worst air quality in the world: Wildfire smog smothers New York. Retrieved from https://www.rmets.org/metmatters/worst-air-quality-world-wildfire-smog-smothers-new-york

Gelaro, R., McCarty, W., Suárez, M. J., Todling, R., Molod, A., Takacs, L., et al. (2017). The modern-era retrospective analysis for research and applications, version 2 (MERRA-2) [Dataset]. *Journal of Climate*, *30*(14), 5419–5454. https://doi.org/10.1175/JCLI-D-16-0758.1

Hanes, C. C., Jain, P., Wang, W., Wang, X., Parisien, M.-A., Little, J. M., & Flannigan, M. D. (2025). Fire regime changes in Canada: An update. *Canadian Journal of Forest Research*, *55*, 1–11. https://doi.org/10.1139/cjfr-2025-0209

Hersbach, H., Bell, B., Berrisford, P., Hirahara, S., Horányi, A., Muñoz-Sabater, J., et al. (2020). The ERA5 global reanalysis [Dataset]. *Quarterly Journal of the Royal Meteorological Society*, *146*(730), 1999–2049. https://doi.org/10.1002/qj.3803

Jain, P., Barber, Q. E., Taylor, S. W., Whitman, E., Castellanos Acuna, D., Boulanger, Y., et al. (2024). Drivers and impacts of the record-breaking 2023 wildfire season in Canada. *Nature Communications*, *15*(1), 6764. https://doi.org/10.1038/s41467-024-51154-7

Kelesidis, G. A., Moularas, C., Parhizkar, H., Calderon, L., Tsiodra, I., Mihalopoulos, N., et al. (2025). Radiative cooling in New York/New Jersey metropolitan areas by wildfire particulate matter emitted from the Canadian wildfires of 2023. *Communications Earth and Environment*, *6*(1), 304. https://doi.org/10.1038/s43247-025-02214-3

Keywood, M., Cope, M., Meyer, C. M., Iinuma, Y., & Emmerson, K. (2015). When smoke comes to town: The impact of biomass burning smoke on air quality. *Atmospheric Environment*, *121*, 13–21. https://doi.org/10.1016/j.atmosenv.2015.03.050

Kochanski, A. K., Mallia, D. V., Fearon, M. G., Mandel, J., Souri, A. H., & Brown, T. (2019). Modeling wildfire smoke feedback mechanisms using a coupled fire-atmosphere model with a radiatively active aerosol scheme. *Journal of Geophysical Research: Atmospheres*, *124*(16), 9099–9116. https://doi.org/10.1029/2019jd030558

Li, F., Zhang, X., Kondragunta, S., Lu, X., Csiszar, I., & Schmidt, C. C. (2022). Hourly biomass burning emissions product from blended geostationary and polar-orbiting satellites for air quality forecasting applications [Dataset]. *Remote Sensing of Environment*, *281*. https://doi.org/10.1016/j.rse.2022.113237

Magaritz-Ronen, L., Menachem, Y., Shafir, A., Maor, S., & Raveh-Rubin, S. (2025). Origin of smoke in the record-breaking air-pollution event in New York, June 2023. *Atmospheric Science Letters*, *26*(6), e1306. https://doi.org/10.1002/asl.1306

Matz, C. J., Egyed, M., Xi, G., Racine, J., Pavlovic, R., Rittmaster, R., et al. (2020). Health impact analysis of PM2.5 from wildfire smoke in Canada (2013–2015, 2017–2018). *Science of the Total Environment*, *725*, 138506. https://doi.org/10.1016/j.scitotenv.2020.138506

Meek, H. C., Aydin-Ghormoz, H., Bush, K., Muscatiello, N., McArdle, C. E., Weng, C. X., et al. (2023). *Notes from the field:* Asthma-associated emergency department visits during a wildfire smoke event—New York, June 2023. MMWR. *Morbidity and Mortality Weekly Report*, *72*(34), 933–935. https://doi.org/10.15585/mmwr.mm7234a6

Randles, C. A., da Silva, A. M., Buchard, V., Colarco, P. R., Darmenov, A., Govindaraju, R., et al. (2017). The MERRA-2 aerosol reanalysis, 1980 onward. Part I: System description and data assimilation evaluation. *Journal of Climate*, *30*(17), 6823–6850. https://doi.org/10.1175/JCLI-D-16-0609.1

Reid, C. E., Brauer, M., Johnston, F. H., Jerrett, M., Balmes, J. R., & Elliott, C. T. (2016). Critical review of health impacts of wildfire smoke exposure. *Environmental Health Perspectives*, *124*(9), 1334–1343. https://doi.org/10.1289/ehp.1409277

Rémy, S., Veira, A., Paugam, R., Sofiev, M., Kaiser, J. W., Marenco, F., et al. (2017). Two global data sets of daily fire emission injection heights since 2003 [Dataset]. *Atmospheric Chemistry and Physics*, *17*(4), 2921–2942. https://doi.org/10.5194/acp-17-2921-2017

Sapkota, A., Symons, J. M., Kleissl, J., Wang, L., Parlange, M. B., Ondov, J., et al. (2005). Impact of the 2002 Canadian forest fires on particulate matter air quality in Baltimore city. *Environmental Science and Technology*, *39*(1), 24–32. https://doi.org/10.1021/es035311z

Shrestha, B., Brotzge, J. A., & Wang, J. (2022). Observations and impacts of long-range transported wildfire smoke on air quality across New York State during July 2021. *Geophysical Research Letters*, *49*(19), e2022GL100216. https://doi.org/10.1029/2022GL100216

Shrestha, B., Brotzge, J. A., Wang, J., Bain, N., Thorncroft, C. D., Joseph, E., et al. (2021). Overview and applications of the New York State Mesonet profiler network [Dataset]. *Journal of Applied Meteorology and Climatology*. https://doi.org/10.1175/JAMC-D-21-0104.1

Sitnov, S. A., Mokhov, I. I., Gorchakov, G. I., & Dzhola, A. V. (2017). Smoke haze over the European part of Russia in the summer of 2016: A link to wildfires in Siberia and atmospheric circulation anomalies. *Russian Meteorology and Hydrology*, *42*(8), 518–528. https://doi.org/10.3103/S1068373917080052

Sofiev, M., Ermakova, T., & Vankevich, R. (2012). Evaluation of the smoke-injection height from wild-land fires using remote-sensing data. *Atmospheric Chemistry and Physics*, *12*(4), 1995–2006. https://doi.org/10.5194/acp-12-1995-2012

Sprenger, M., & Wernli, H. (2015). The LAGRANTO Lagrangian analysis tool—Version 2.0 [Software]. *Geoscientific Model Development*, *8*(8), 2569–2586. https://doi.org/10.5194/gmd-8-2569-2015

Su, J., Delgado, R., Berkoff, T. A., Sullivan, J. T., Gronoff, G. P., & Phoenix, D. B. (2025). Observation of fresh wildfire smoke over Hampton, VA in winter. *Atmospheric Environment*, *358*, 121370. https://doi.org/10.1016/j.atmosenv.2025.121370

Wang, Z., Huang, X., Xue, L., Ding, K., Lou, S., Zhu, A., & Ding, A. (2024). Intensification of mid-latitude cyclone by aerosol-radiation interaction increases transport of Canadian wildfire smoke to Northeastern US. *Geophysical Research Letters*, *51*(13), e2024GL108444. https://doi.org/10.1029/2024GL108444

Wang, Z., Wang, Z., Zou, Z., Chen, X., Wu, H., Wang, W., et al. (2024). Severe global environmental issues caused by Canada's record-breaking wildfires in 2023. *Advances in Atmospheric Sciences*, *41*(4), 565–571. https://doi.org/10.1007/s00376-023-3241-0

Zheng, G., Sedlacek, A. J., Aiken, A. C., Feng, Y., Watson, T. B., Raveh-Rubin, S., et al. (2020). Long-range transported north American wildfire aerosols observed in marine boundary layer of eastern north Atlantic. *Environment International*, *139*, 105680. https://doi.org/10.1016/j.envint.2020.105680

Zhu, Y., Hsu, P., & Qian, Y. (2024). Influence of Western Pacific Madden–Julian oscillation on New York City's record-breaking air pollution in early June 2023. *Geophysical Research Letters*, *51*(14), e2024GL109061. https://doi.org/10.1029/2024GL109061

Zu, K., Tao, G., Long, C., Goodman, J., & Valberg, P. (2016). Long-range fine particulate matter from the 2002 Quebec forest fires and daily mortality in Greater Boston and New York City. *Air Quality, Atmosphere and Health*, *9*(3), 213–221. https://doi.org/10.1007/s11869-015-0332-9

References From the Supporting Information

Adler, R. F., Huffman, G. J., Chang, A., Ferraro, R., Xie, P.-P., Janowiak, J., et al. (2003). The version-2 global precipitation climatology project (GPCP) monthly precipitation analysis (1979–present). *Journal of Hydrometeorology*, *4*(6), 1147–1167. https://doi.org/10.1175/1525-7541(2003)004⟨1147:TVGPCP⟩2.0.CO;2